

DESY 04-077
IFT-04/10
MC-TH-2004-02
PSI-PR-04-06
hep-ph/0404119

Determining $\tan\beta$ in $\tau\tau$ Fusion to SUSY Higgs Bosons at a Photon Collider

S. Y. Choi¹, J. Kalinowski², J.S. Lee³, M.M. Mühlleitner⁴, M. Spira⁴
and P. M. Zerwas⁵

¹ Dept. Physics, Chonbuk National University, Chonju 561-756, Korea

² Inst. Theor. Physics, Warsaw University, PL-00681 Warsaw, Poland

³ Dept. Physics and Astronomy, Univ. Manchester, Manchester M13 9PL, UK

⁴ Paul Scherrer Institut, CH-5232 Villigen PSI, Switzerland

⁵ Deutsches Elektronen-Synchrotron DESY, D-22603 Hamburg, Germany

Abstract

We investigate $\tau\tau$ fusion to light h and heavy H and A Higgs bosons in the Minimal Supersymmetric Standard Model (MSSM) at a photon collider as a promising channel for measuring large values of $\tan\beta$. For standard design parameters of a photon collider an error $\Delta\tan\beta \sim 1$, uniformly for $\tan\beta \gtrsim 10$, may be expected, improving on complementary measurements at the LHC and e^+e^- linear colliders.

1. Introduction. The measurement of the mixing parameter $\tan\beta$, one of the fundamental parameters in the Higgs sector of the Minimal Supersymmetric Standard Model (MSSM) and other supersymmetric scenarios, is a difficult task. Many of the observables, in the chargino/neutralino sector [1] for instance, involve only $\cos 2\beta$, the slope of which approaches $-4/\tan^3\beta$ for large values of $\tan\beta$ and thus are quite insensitive to the parameter $\tan\beta$ in this range. Remarkably different however are the heavy H/A Higgs couplings to down-type fermions which, for values of the pseudoscalar Higgs boson mass at the electroweak scale and beyond, both are directly proportional to $\tan\beta$ if this parameter becomes large, see *e.g.* Ref. [2], and which thus are highly sensitive to its value. Also the down-type couplings of the light h Higgs boson in the MSSM are close to $\tan\beta$ if the pseudoscalar mass is moderately small.

The Higgs down-type fermion vertices play a decisive role in various observables which can be exploited for measuring $\tan\beta$. Examples are the total widths of the H/A Higgs bosons [3], Higgs-bremsstrahlung off bottom quarks in e^+e^- collisions [4], and polarization effects [5]. A summary of the expected results has been presented recently in Ref. [6]. Moreover, b -quark fusion to H/A bosons at the LHC has recently been investigated in a detailed experimental simulation [7] and proved quite promising for large values of $\tan\beta$. All these methods are applicable in part of the MSSM parameter space and expected accuracies generally hover around the 10% level. In this situation any additional method for measuring $\tan\beta$ is valuable, improving the picture significantly even if the individual error remains of similar size.

In this note we point out that $\tau\tau$ fusion to Higgs bosons at a photon collider can provide a valuable method for measuring $\tan\beta$ – a natural next step after searching for Higgs bosons in $\gamma\gamma$ fusion [8] and exploiting the associated loop-induced production cross section [9]. The entire Higgs mass range can be covered by this method up to the kinematical limit for large $\tan\beta$.

In the next section a semi-quantitative analytical discussion of $\tau\tau$ fusion to Higgs bosons will motivate the detailed study. The fusion process is the dominant Higgs boson production process in $\gamma\gamma$ collisions giving rise to $\tau^+\tau^- + \text{Higgs}$ in the final state. In the subsequent numerical analysis, however, a full set of signal and background processes is taken into account. We demonstrate that for standard design parameters of a photon collider an error $\Delta \tan\beta \sim 1$ in measurements of a large $\tan\beta$ value can be expected.

2. $\tau\tau$ Fusion at a Photon Collider. The alternative channel to the methods summarized above, $\tau\tau$ fusion to the light and heavy $h/H/A$ Higgs bosons at a photon collider, *cf.* Fig.1, is based on the two-step process:

$$\gamma + \gamma \rightarrow (\tau^+\tau^-) + (\tau^+\tau^-) \rightarrow \tau^+\tau^- + h/H/A \quad (1)$$

For the large- $\tan\beta$ case studied here in detail as an example – the Higgs-mass slope crossing the Snowmass point SPS1b [10] – the decay channels of Higgs bosons to supersymmetric particles are nearly shut and all the Higgs bosons $\Phi = h/H/A$ decay almost exclusively, *i.e.* 80 to 90%, to a pair of b quarks. Therefore the final state consists of a pair of τ 's and a pair of resonant b quark jets.

Unlike LHC, $\tau\tau$ fusion is superior to b -quark fusion at a photon collider. This is apparent from a quick estimate of the charges and couplings involved. b -quark fusion is suppressed by the fractional electric charge $e_b = -1/3$ that cannot be compensated by color nor by the enhancement of the fermion-Higgs Yukawa coupling. In total, the b -channel suppression is of order $3(1/3)^4(m_b/m_\tau)^2 \sim 0.1$ compared with the tau channel.

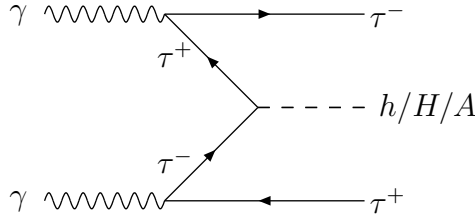


Figure 1: The process of $\tau\tau$ fusion to Higgs bosons in $\gamma\gamma$ collisions.

Energies in the range of more than one hundred GeV, *i.e.* the size of the Higgs-boson masses, quite naturally suggest the application of the equivalent-particle approximation to the $\gamma\gamma$ process (1). In this approximation, the process can be decomposed into two consecutive steps: photon splittings to tau pairs, $\gamma \rightarrow \tau^+\tau^-$, followed by the fusion process of two (almost on-shell) taus to the Higgs bosons, $\tau^+\tau^- \rightarrow \Phi$, *cf.* Fig. 1. Hence, the cross section is given by the convolution of the fusion cross section with the $\tau\tau$ luminosity in the colliding photon beams.

The fusion cross section to the Higgs bosons Φ may be written

$$\hat{\sigma}[\tau^+\tau^- \rightarrow \Phi; \hat{s}] = \frac{\pi m_\tau^2}{2v^2} g_{\Phi\tau\tau}^2 \frac{M_\Phi \Gamma_\Phi / \pi}{(\hat{s} - M_\Phi^2)^2 + M_\Phi^2 \Gamma_\Phi^2} \quad (2)$$

where \hat{s} denotes the $\tau^+\tau^-$ invariant energy squared and v is the Higgs vacuum expectation value, $v \simeq 246$ GeV. The coupling $g_{\Phi\tau\tau}$ is normalized to the Standard Model Higgs coupling to a tau pair, m_τ/v . For large $\tan\beta$, the couplings^a are given by

$$\begin{aligned} g_{\Phi\tau\tau} &= \tan\beta & \text{for } \Phi = A \\ g_{\Phi\tau\tau} &\simeq \tan\beta & \text{for } \Phi = h, H \end{aligned} \quad (3)$$

if the pseudoscalar mass parameter M_A is sufficiently light in the case of h , and sufficiently heavy in the case of H , *cf.* Ref. [2] for details. The $\tau\tau$ luminosity can be derived from the $\gamma \rightarrow \tau$ structure function [11]

$$D_\gamma^\tau(z) = \frac{\alpha}{2\pi} [z^2 + (1-z)^2] \log \frac{\mu_F^2}{m_\tau^2} \quad (4)$$

^aNote that in contrast to the b -quark couplings, the τ -couplings are not strongly renormalized by higher-order corrections.

where the energy fraction transferred from γ to τ is denoted by z and non-logarithmic terms have been neglected. The factorization scale μ_F typical for the subsequent fusion process is set by the Higgs mass in this calculation, $\mu_F = M_\Phi$.

From these two elements the total $\gamma\gamma$ cross section can be calculated in the narrow-width approximation as

$$\sigma[\gamma\gamma \rightarrow \tau^+\tau^-\Phi] = \frac{\pi m_\tau^2}{2v^2 s} g_{\Phi\tau\tau}^2 \times 2 \int_\tau^1 \frac{dz}{z} D_\gamma^\tau(z) D_\gamma^\tau(\tau/z) \quad (5)$$

where $\tau = M_\Phi^2/s$, with s being the c.m. energy squared of the photons. Defining the $\tau\tau$ luminosity function by the convolution integral of the structure functions (including the multiplicity factor 2), the leading-logarithmic part, F_{LL} , is given by

$$\begin{aligned} F_{LL}(\tau) &= \left(\frac{\alpha}{2\pi}\right)^2 f_{LL}(\tau) \log^2 \frac{M_\Phi^2}{m_\tau^2} \\ f_{LL}(\tau) &= 2(1+2\tau)^2 \log \tau^{-1} - 4(1-\tau)(1+3\tau) \end{aligned} \quad (6)$$

The single log corrections can be included by replacing $F_{LL} \rightarrow F_{LL} + F_L$ where^b

$$\begin{aligned} F_L(\tau) &= \left(\frac{\alpha}{2\pi}\right)^2 f_L(\tau) \log \frac{M_\Phi^2}{m_\tau^2} \\ f_L(\tau) &= -8(1-\tau)(1+3\tau) \log(1-\tau) + (1+2\tau)^2 [\log^2 \tau + 4Li_2(\tau) - \frac{2\pi^2}{3}] \\ &\quad - (5 + 24\tau + 4\tau^2) \log \tau^{-1} + \frac{1}{2}(1-\tau)(27 + 103\tau) \end{aligned} \quad (7)$$

Fig. 2 displays the luminosity function in the leading logarithmic approximation, F_{LL} , and corrected with the single log, $F_{LL} + F_L$. Adding to the luminosity function the corrections from Higgs bremsstrahlung off the external τ legs in the $\gamma\gamma$ process, the generalized function $F(\tau)$, defined in parallel to the split form of Eq.(5) and calculated in the next section, is shown here for comparison^c. Evidently, the analytical calculations provide us with a good-quality picture of the process so that a proper understanding of the mechanisms involved can be claimed.

For energies sufficiently above threshold, F_{LL} provides a solid basis for estimating the cross sections. The analytical formula Eq.(6) can readily be used therefore for a first estimate of the potential for measuring $\tan\beta$ in the $b\bar{b}$ -decay channel. A rough estimate shows the size of the cross section to be ~ 8 fb for the $\gamma\gamma$ c.m. energy $E_{\gamma\gamma} = 600$ GeV, $M_{H/A} = 400$ GeV and $\tan\beta = 30$. For an integrated luminosity of 200 fb^{-1} , which may be accumulated in running the $\gamma\gamma$ collider for one year, about 3000 events can be expected in both H and A decay channels. As a result, a statistical error of order 1% can be predicted that compares favorably well with other methods [6, 7]. On the other hand the light Higgs boson h and the heavy Higgs bosons H, A for moderate mass values can also be produced at lower energies, *e.g.* $E_{\gamma\gamma} = 400$ GeV.

^bFor a general factorization scale $\mu_F \neq M_\Phi$, the term $2f_{LL} \log \mu_F^2/M_\Phi^2$ must be subtracted from f_L in Eq.(7).

^cThis discussion has also been presented in some detail as it sheds light on the quality of the parton picture for heavy quarks in high-energy proton beams where comparisons cannot be performed with the same rigor as in the lepton sector.

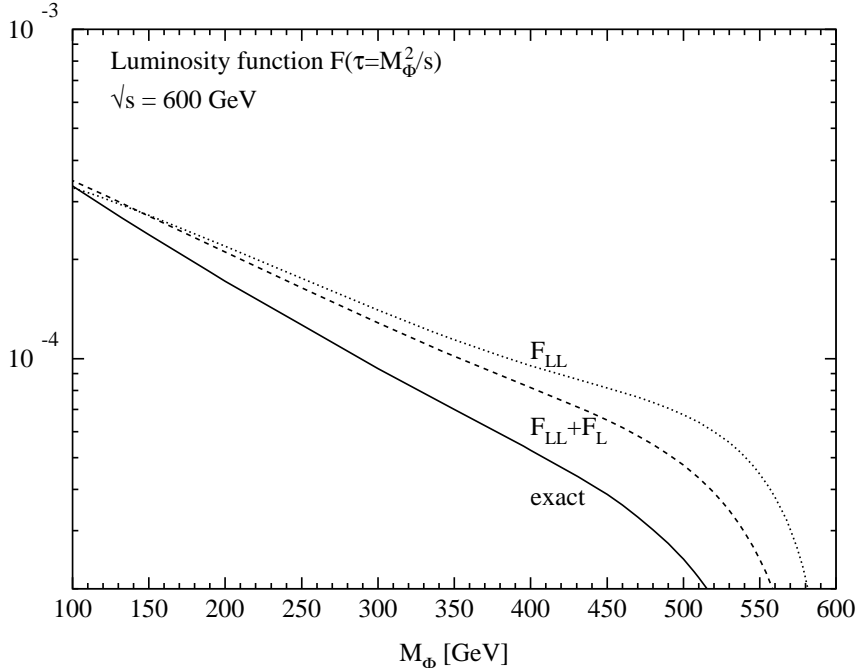


Figure 2: Comparison of the luminosity function F calculated in the leading-log approximation, F_{LL} , corrected with the single log, $F_{LL} + F_L$, and the exact tree-level calculation, presented as functions of the Higgs boson mass M_Φ .

In the same way we can estimate the size of the cross section for the main background channel: $\tau^+\tau^-$ annihilation into a pair of b -quarks, $\tau^+\tau^- \rightarrow b\bar{b}$, via s -channel γ and Z exchanges, Fig. 3 left panel. As the mechanism is electroweak, the cross section is naturally small (what would have been different for $4b$ final states where strong QCD processes would be activated). If proper care is taken for the invariant mass of any of the fermion pairs not to match the Z -boson mass (except for h), the transition probability is reduced by one power of the electroweak coupling squared compared with the signal process. The $\gamma\gamma$ cross section of this background channel is obtained by integrating the parton cross section $\hat{\sigma}[\tau^+\tau^- \rightarrow \gamma, Z \rightarrow b\bar{b}] = 4\pi\alpha^2 \langle |Q_b Q_\tau|^2 \rangle / \hat{s}$, with the familiar generalized electroweak charges Q_τ and Q_b , over the $\tau\tau$ luminosity of the $\gamma\gamma$ collider within the range Δ at the invariant energy $\sqrt{\hat{s}} = M_\Phi$. The integration range Δ is taken either as the total width of the Higgs bosons Γ_Φ or as the estimated experimental resolution $\Delta_{ex} \simeq \pm 0.05 M_\Phi$ of the $b\bar{b}$ final state [12]:

$$\Delta = \max[\Gamma_\Phi, 2\Delta_{ex}] \quad (8)$$

Inserting typical parameters for a Higgs boson mass of $M_{H/A} = 400$ GeV, one finds a background cross section of size $\lesssim 5 \times 10^{-3}$ fb. This value, corresponding roughly to the signal for $\tan\beta \sim 2$, is much smaller than the size of the signal cross section for large values of $\tan\beta \gtrsim 10$. Similar signal-to-background ratios are predicted for the light Higgs boson h , except for masses close to the Z -boson mass. For small Higgs-boson masses,

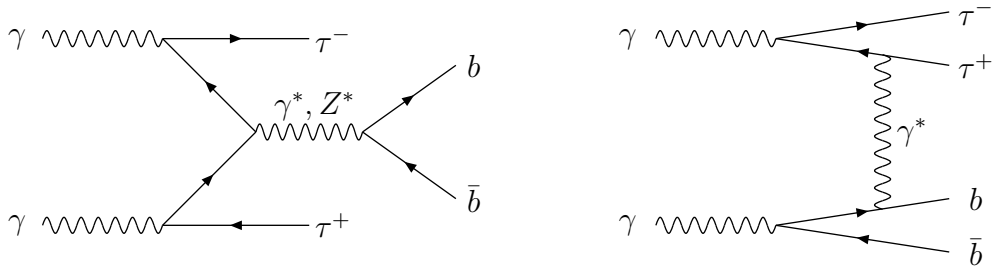


Figure 3: The annihilation and diffractive background processes in $\gamma\gamma$ collisions giving rise to $\tau\tau b\bar{b}$ final states.

the background gradually increases when the $b\bar{b}$ invariant mass approaches the on-shell Z -boson mass and the background suppression as a result of the additional electroweak coupling ceases to be effective.

The topology of the related background process of $b\bar{b}$ fusion to a $\tau^+\tau^-$ pair via γ or Z exchange is quite different from the signal. It can be suppressed to a very small level in two ways: by requiring sufficiently large transverse momenta of the b quarks and sufficiently small transverse momenta for the τ 's.

A second background channel is associated with diffractive $\gamma\gamma \rightarrow (\tau^+\tau^-)(b\bar{b})$ events, the pairs scattering off each other by Rutherford photon exchange, Fig. 3 right panel. While being very large in principle, the diffractive background can be suppressed strongly by proper cuts. The paired fermions in diffractive events travel preferentially parallel to the γ axes and they carry small invariant mass. Requiring therefore a large invariant mass for the $b\bar{b}$ pair, equivalent to the Higgs signal, and, as suggested by the topology of the signal, the τ 's to go into opposite directions near the beam axis, the background can be reduced strongly. This expectation is borne out by the quantitative numerical analysis presented in the next section.

3. Numerical Analysis. Encouraged by the semi-quantitative estimates, we have performed a detailed numerical analysis for signal and backgrounds.

Assuming an $e^\pm e^-$ collider c.m. energy of 800 GeV, the maximum of $\gamma\gamma$ energy spectrum can be taken as 600 GeV. Adopting the TESLA parameters, for instance, an integrated $\gamma\gamma$ luminosity of about 200 fb^{-1} *per annum* can be expected in the margin 20% below the maximum e^+e^- energy [13]. Similarly, about 100 fb^{-1} may be accumulated for a $\gamma\gamma$ energy of 400 GeV at a 500 GeV $e^\pm e^-$ collider.

As alluded to before, we shall analyze the system under the assumption that Higgs decay channels to supersymmetric particles are shut. Such a scenario is realized approximately in the Snowmass reference point SPS1b [10] for which decays to charginos and neutralinos add up to a branching ratio of less than 1%, see Fig. 4. In this situation the H/A Higgs bosons decay primarily to $b\bar{b}$ pairs with a small admixture of $\tau\tau$ pairs for large $\tan\beta$: $BR_\tau/BR_b = 1/3 (m_\tau/m_b)^2 \sim 0.1$ for Higgs masses of 400 GeV. The H/A decay

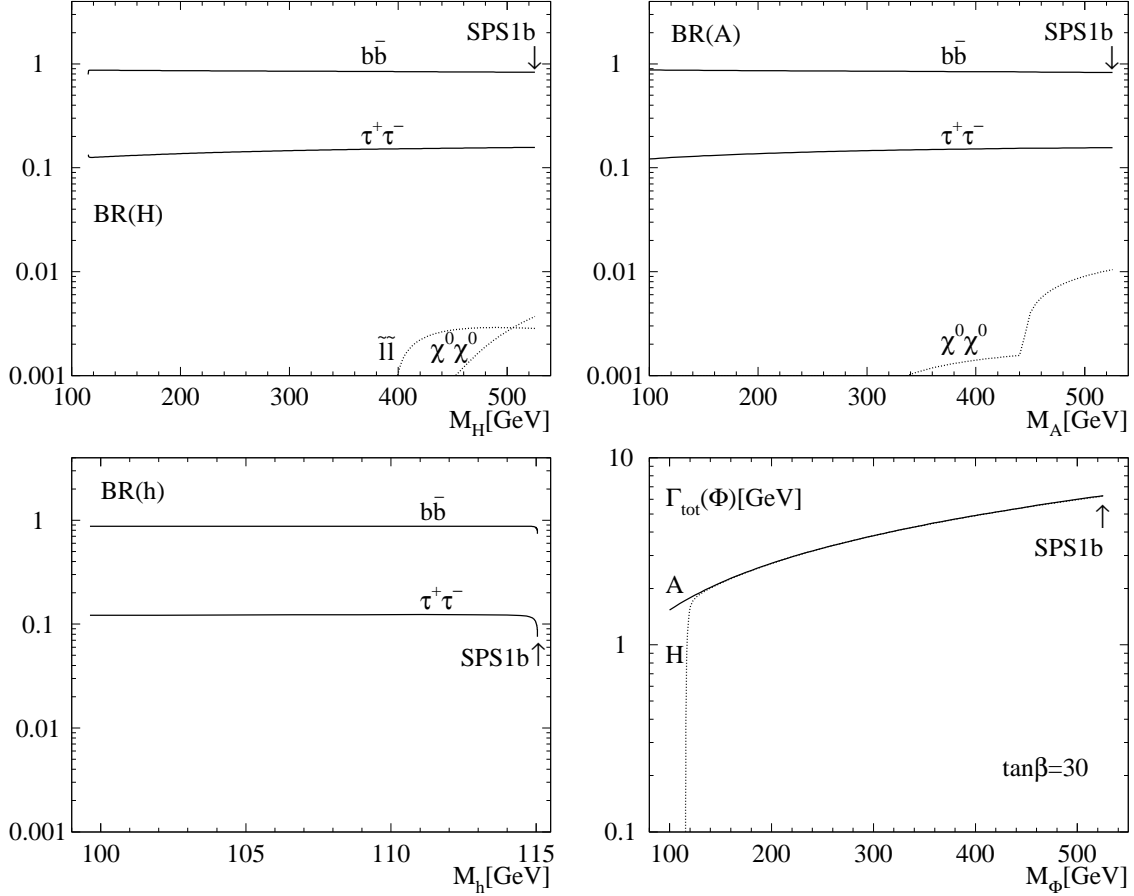


Figure 4: The decay branching ratios of the Higgs bosons H and A (upper row) and h (lower left). The lower right panel shows the total decay widths of H and A . All quantities are given as functions of the respective Higgs boson mass. The SUSY parameters, in particular $\tan\beta = 30$, have been chosen as in the SPS1b scenario except for M_A which varies from 100 GeV to 525 GeV. The upper limit corresponds to the SPS1b Snowmass point.

widths, which are important parameters to control the background suppression, are also shown in Fig. 4 for $\tan\beta = 30$ as a function of the Higgs masses. In the mass range of interest the total Higgs decay widths are of the order of a few GeV. Moreover, they are comparable to the experimental $b\bar{b}$ invariant mass resolution, and the resonant b -quark jets from the Higgs boson decay should clearly be visible above the smooth background. The light Higgs boson h has similar decay branching ratios for moderately small M_A .

In the numerical analysis the full set of diagrams for the signal processes $\gamma\gamma \rightarrow \tau^+\tau^- + \Phi[\rightarrow b\bar{b}]$ and all diagrams for the background processes $\gamma\gamma \rightarrow \tau^+\tau^- b\bar{b}$, generated by means of CompHEP [14], are taken into account. This set includes for the signal in particular bremsstrahlung of the Higgs bosons off the external τ legs in the non-logarithmic corrections to the equivalent-particle approximation.

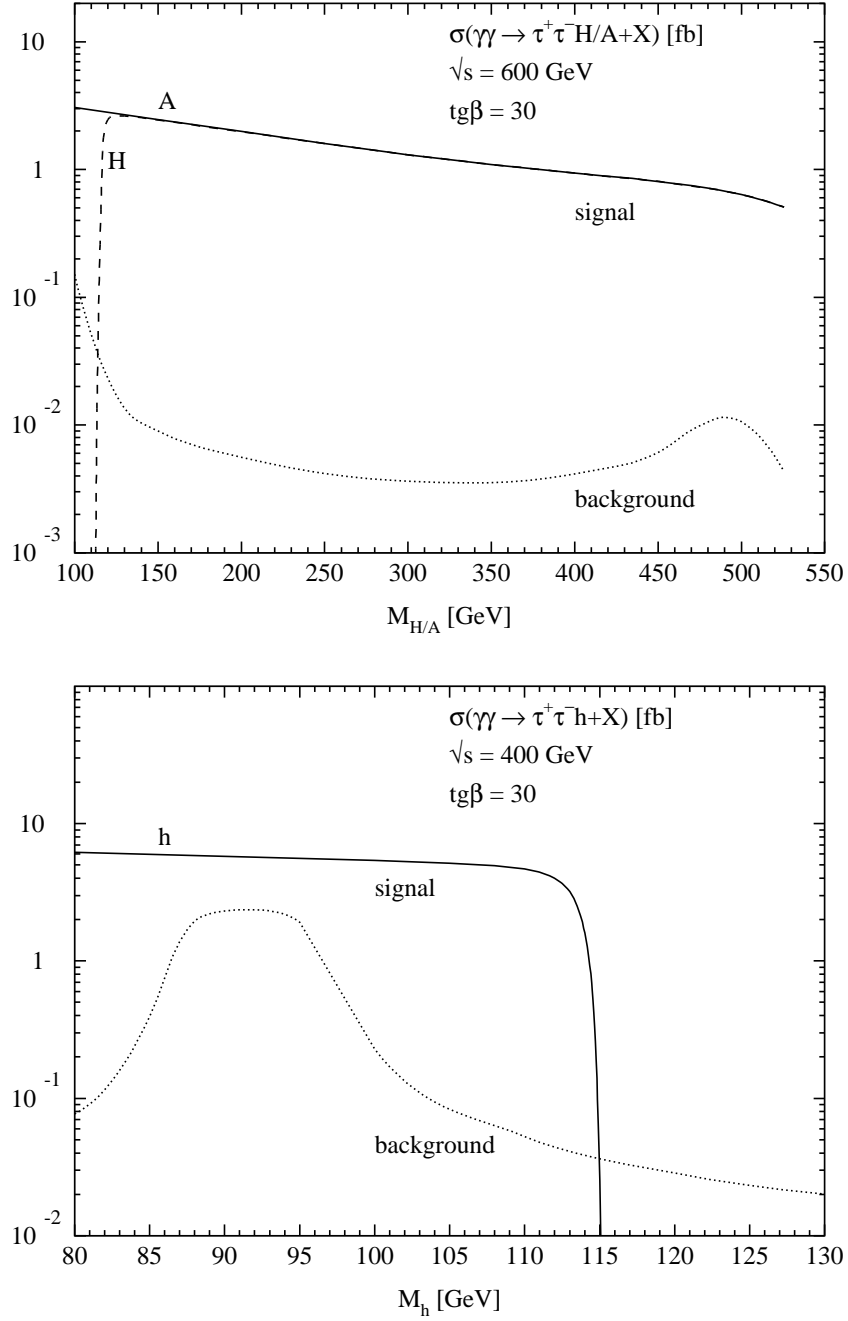


Figure 5: The cross sections for the production of the H/A (top) and h (bottom) Higgs bosons in the $\tau\tau$ fusion process for $\tan\beta = 30$. Also shown is the background cross section for experimental cuts as specified in the text. SUSY parameters as in Fig.4. \sqrt{s} denotes the $\gamma\gamma$ collider c.m. energy, corresponding to approximately 80% of the $e^\pm e^-$ linear collider energy.

We finally present in the top panel of Fig. 5 the exact cross sections for the signals coming from the production of H and A Higgs bosons in the $\tau\tau$ fusion process together with all the background processes. The cuts which define the final states have been chosen such that the diffractive γ -exchange mechanism is suppressed sufficiently well. For this purpose, the invariant $b\bar{b}$ mass has been constrained to the bracket Δ as defined in Eq.(8)^d, the taus are assumed visible and traveling in opposite directions to the beam axis with tau energies in excess of 5 GeV and polar angles beyond 130 mrad to account for the shielding. Note that no cut on the $\tau^+\tau^-$ invariant mass is required to suppress the $b\bar{b}$ fusion process to Z bosons decaying to τ pairs which increases the background cross section marginally for large Higgs masses before it is cut off completely by phase space. Even $\tan\beta$ values down to $\tan\beta \gtrsim 5$ could be probed without running into background problems. [The discussion of experimental cuts on transverse momenta and total event energy to remove overlaying $\gamma\gamma$ events is beyond the scope of this theoretical study.]

In the complementary bottom panel of Figure 5 it is shown that also $\tau\tau$ fusion to the light Higgs boson h can be exploited to measure $\tan\beta$ for large values if the pseudoscalar mass is moderately small. In the example presented in Fig. 5, the $\gamma\gamma$ c.m. energy has been set to 400 GeV.

The drop in the H and h signal cross sections at the lower and upper end of the mass range, respectively, is caused by the reduction of the $H\tau\tau$ and $h\tau\tau$ couplings to the Standard Model values in these parameter areas.

	$E_{\gamma\gamma} = 400 \text{ GeV}, \mathcal{L} = 100 \text{ fb}^{-1}$			$E_{\gamma\gamma} = 600 \text{ GeV}, \mathcal{L} = 200 \text{ fb}^{-1}$				
	$A \oplus h$	$A \oplus H$		$A \oplus h$	$A \oplus H$			
M_{Higgs} [GeV]	100	200	300	100	200	300	400	500
$\tan\beta$	I	II	III	IV	V	VI	VII	VIII
10	8.4%	10.7%	13.9%	8.0%	9.0%	11.2%	13.2%	16.5%
30	2.6%	3.5%	4.6%	2.4%	3.0%	3.7%	4.4%	5.3%
50	1.5%	2.1%	2.7%	1.5%	1.8%	2.2%	2.6%	3.2%

Table 1: Relative errors $\Delta \tan\beta / \tan\beta$ on $\tan\beta$ measurements for $\tan\beta = 10, 30$ and 50 based on: combined $A \oplus h$ [I,IV] and $A \oplus H$ [II,III,V-VIII] production, assuming $E_{\gamma\gamma} = 400 \text{ GeV}, \mathcal{L} = 100 \text{ fb}^{-1}$ and $E_{\gamma\gamma} = 600 \text{ GeV}, \mathcal{L} = 200 \text{ fb}^{-1}$. Cuts and efficiencies are applied on the final-state τ 's and b jets as specified in the text.

The statistical accuracy with which large $\tan\beta$ values can be measured in $\tau\tau$ fusion to Higgs bosons can be estimated from the predicted cross sections and the assumed integrated luminosities. Efficiencies for $b\bar{b}$ tagging, $\epsilon_{b\bar{b}}$, and $\tau\tau$ tagging, $\epsilon_{\tau\tau}$, reduce the accuracies. For $\epsilon_{b\bar{b}} \sim 0.7$ and $\epsilon_{\tau\tau} \sim 0.5$, for example [12], the errors grow by a factor

^dOn the $M_{A,H}$ slope of SPS1b analyzed here in detail, the heavy Higgs bosons remain so narrow that Δ is always given by the experimental resolution Δ_{ex} .

$1/\sqrt{\epsilon_{bb}\epsilon_{\tau\tau}} \sim 1.7$. The expected errors for $h/H/A$ production are exemplified for three $\tan\beta$ values, $\tan\beta = 10, 30$ and 50 , in Table 1. The integrated luminosities are chosen to be 200 fb^{-1} for the high energy option and 100 fb^{-1} for the low energy option [13]. For h production, the mass parameters are set to $M_A \sim 100 \text{ GeV}$ and $M_h = 100 \text{ GeV}$; for the production of the heavy pseudoscalar A the mass is varied between 100 and 500 GeV. Results for scalar H production are identical to A in the mass range above 120 GeV. The two channels h and A , and H and A are combined in the overlapping mass ranges in which the two states, respectively, cannot be discriminated. In Table 1 we have presented the relative errors $\Delta \tan\beta / \tan\beta$. Since in the region of interest the $\tau\tau$ fusion cross sections are proportional to $\tan^2\beta$ and the background is small, the absolute errors $\Delta \tan\beta$ are nearly independent of $\tan\beta$, varying between

$$\Delta \tan\beta \simeq 0.9 \quad \text{and} \quad 1.3 \tag{9}$$

for Higgs mass values away from the kinematical limits.

It should be noted that away from the kinematical limits, the Higgs fusion cross sections $\sim F/s$, Eq.(5), vary little with the $\gamma\gamma$ energy since the suppression by s is almost compensated by the luminosity function F . As a result, the smearing of the $\gamma\gamma$ energy has a mild effect on the analysis presented here. Moreover, since the $\gamma\gamma$ luminosity rises with the collider energy, the errors on $\tan\beta$ decrease. Of course, detailed experimental simulations are required for the final conclusions on the anticipated accuracies. However, the above estimates can clearly be interpreted as encouraging experimental simulations with promising prospects for valuable measurements of $\tan\beta$.

4. Summary. We have demonstrated in this letter that $\tau\tau$ fusion to the heavy Higgs bosons H/A of the MSSM at a photon collider is a promising channel for measuring the Higgs mixing parameter $\tan\beta$ at large values. Complemented by $\tau\tau$ fusion to the light Higgs boson h for moderately small values of the pseudoscalar Higgs boson mass M_A , the MSSM parameter range can nicely be covered in all scenarios. The analysis compares favorably well with the corresponding b -quark fusion process at the LHC [7]. Moreover, the method can be applied readily for a large range of Higgs mass values and thus is competitive with complementary methods in the e^+e^- mode of a linear collider [6].

Acknowledgments: We thank K. Desch and V. Telnov for valuable advise on experimental parameters relevant for this study. Remarks on the manuscript by K. Desch, M. Krawczyk and D. Rainwater are gratefully acknowledged.

The work is supported in part by the European Commission 5-th Framework Contract HPRN-CT-2000-00149. The work of SYC was supported in part by the Korea Research Foundation Grant (KRF-2002-070-C00022) and in part by KOSEF through CHEP at Kyungpook National University. JK was supported by the KBN Grant 2 P03B 040 24 (2003-2005) and 115/E-343/SPB/DESY/P-03/DWM517/2003-2005. The work of JSL was supported in part by PPARC. MMM and MS have been supported in part by the Swiss Bundesamt für Bildung und Wissenschaft.

References

- [1] S. Y. Choi, A. Djouadi, M. Guchait, J. Kalinowski, H. S. Song and P. M. Zerwas, *Eur. Phys. J. C* **14** (2000) 535 [arXiv:hep-ph/0002033]; S. Y. Choi, J. Kalinowski, G. Moortgat-Pick and P. M. Zerwas, *Eur. Phys. J. C* **22** (2001) 563 [Addendum-ibid. *C* **23** (2002) 769] [arXiv:hep-ph/0108117]; K. Desch, J. Kalinowski, G. Moortgat-Pick, M. M. Nojiri and G. Polesello, *JHEP* **0402** (2004) 035 [arXiv:hep-ph/0312069].
- [2] M. Spira and P. M. Zerwas, Lectures at the Schladming Winter School 1997 [arXiv:hep-ph/9803257]; E. Boos, A. Djouadi, M. Mühlleitner and A. Vologdin, *Phys. Rev. D* **66** (2002) 055004 [arXiv:hep-ph/0205160].
- [3] J. F. Gunion, T. Han, J. Jiang and A. Sopczak, *Phys. Lett. B* **565** (2003) 42 [arXiv:hep-ph/0212151].
- [4] J. Kalinowski and S. Pokorski, *Phys. Lett. B* **219** (1989) 116; A. Djouadi, P. M. Zerwas and J. Zunft, *Phys. Lett. B* **259** (1991) 175; S. Dittmaier, M. Krämer, Y. Liao, M. Spira and P. M. Zerwas, *Phys. Lett. B* **478** (2000) 247 [arXiv:hep-ph/0002035].
- [5] M. M. Nojiri, *Phys. Rev. D* **51** (1995) 6281 [arXiv:hep-ph/9412374]; M. M. Nojiri, K. Fujii and T. Tsukamoto, *Phys. Rev. D* **54** (1996) 6756 [arXiv:hep-ph/9606370]; E. Boos, H. U. Martyn, G. Moortgat-Pick, M. Sachwitz, A. Sherstnev and P. M. Zerwas, *Eur. Phys. J. C* **30** (2003) 395 [arXiv:hep-ph/0303110].
- [6] J. F. Gunion, T. Han, J. Jiang and A. Sopczak, Contribution to the LHC/LC Physics Document, *eds.* R. Godbole, F. Paige and G. Weiglein, April 2004.
- [7] R. Kinnunen, S. Lehti, F. Moortgat, S. Nikitenko and M. Spira, CMS–Note CMS AN 2003/014.
- [8] M. M. Mühlleitner, M. Krämer, M. Spira and P. M. Zerwas, *Phys. Lett. B* **508** (2001) 311 [arXiv:hep-ph/0101083]; M. M. Velasco *et al.*, in *Proc. of the APS/DPF/DPB Summer Study on the Future of Particle Physics (Snowmass 2001)*, *ed.* N. Graf [arXiv:hep-ex/0111055]; D. M. Asner, J. B. Gronberg and J. F. Gunion, *Phys. Rev. D* **67** (2003) 035009.
- [9] P. Niezurawski, A. F. Żarnecki and M. Krawczyk, arXiv:hep-ph/0307180.
- [10] B. C. Allanach *et al.*, in *Proc. of the APS/DPF/DPB Summer Study on the Future of Particle Physics (Snowmass 2001)*, *ed.* N. Graf, *Eur. Phys. J. C* **25** (2002) 113 [arXiv:hep-ph/0202233].
- [11] M. S. Chen and P. M. Zerwas, *Phys. Rev. D* **12** (1975) 187.
- [12] K. Desch, *private communication*.

- [13] B. Badelek *et al.* [ECFA/DESY Photon Collider Working Group Collaboration], TESLA-TDR, Part VI, DESY 02-011 [arXiv:hep-ex/0108012]; E. Boos *et al.*, Nucl. Instrum. Meth. A **472** (2001) 100 [arXiv:hep-ph/0103090].
- [14] A. Pukhov, E. Boos, M. Dubinin, V. Edneral, V. Ilyin, D. Kovalenko, A. Kryukov, V. Savrin, S. Shichanin and A. Semenov, arXiv:hep-ph/9908288.